Proceedings of the ASME 2019 International Mechanical Engineering Congress and Exposition
IMECE2019
November 11-14, 2019, Salt Lake City, UT, USA

IMECE2019-10617

GENETIC ALGORITHM BASED TOPOLOGY OPTIMIZATION OF HEAT EXCHANGER FINS USED IN AEROSPACE APPLICATIONS

Bashir S. Mekki[1], Joshua Langer[2], and Stephen Lynch[3]
Department of Mechanical Engineering
Pennsylvania State University
University Park, PA

ABSTRACT

Topology Optimization (TO) in the design of structural components is commonly used and well explored. However, its usage in the design of complex thermo-fluid equipment used in aerospace applications is limited and relatively new. This is because the coupling between the fluid dynamics, heat transfer, and the shape is complex and nonlinear. Furthermore, the resulting geometry from a TO analysis is often very complex and difficult to manufacture due to the free forms that can occur. With the advent of Additive Manufacturing (AM), however, it has become possible to directly manufacture complex geometries. This study develops a new Genetic Algorithm (GA) based TO combined with Computational Fluid Dynamics (CFD) to produce optimized fin shapes for heat exchangers used in aerospace applications. To implement this approach, a rectangular shaped baseline fin geometry was created using voxel representation. An initial population is generated by mutating the baseline fin a random number of times. The CFD package OpenFOAM is then used to evaluate the performance of each design, after which the optimization algorithm is applied. The GA sorts the designs using a composite fitness function that is comprised of the overall heat transfer and pressure drop, and generates new generations based on mutation and carryover of top performing designs. The study also explores the sensitivity of the GA to the various GA parameters as well as the effect of varying flow Reynolds number. In general, as Reynolds number increases, the percent improvement in the optimum relative to the baseline increases, with potentially a 60% performance improvement. Overall, the approach enables generation of novel freeform designs that may open new performance space for heat transfer applications.

Keywords: Genetic Algorithms (GA), Topology Optimization, Heat Transfer, Offset Strip Fins, Heat Exchangers, Additive Manufacturing (AM).

1. INTRODUCTION

Compact heat exchangers are used in a wide range of applications. Among these is aerospace applications where the need for lightweight, space saving heat exchangers is very critical. This goal can be achieved by improving the heat exchanger efficiency which has been the subject of many studies. The focus of most of these studies was to generate new designs that enhance the heat transfer by introducing a larger surface area and/or increasing convective heat transfer coefficient.

For heat exchangers that use air as one or more of the streams, the low heat transfer coefficient necessitates large surface area which can be accomplished using fins. The search for best performance has led to the introduction of a variety of different configurations such as wavy, offset strip, louvered, pin, and perforated fins[1]. The more complex the geometry, the higher the heat transfer; however, traditional manufacturing limitations can restrict novel geometries that may theoretically offer a very high efficiency but are impossible to manufacture. The advent of additive manufacturing, in addition to the significant improvement in computational tools may produce concepts that have not yet been explored.

Recently, the concept of TO has emerged as a powerful design tool for complex thermo-fluid equipment [2]. It is mainly used in the field of structural analysis to design mechanical parts in which the objective is to minimize the material used while maintaining the same mechanical strength.

The goal of this study is to explore the possibility of combining genetic algorithm-based topology optimization with computational fluid dynamics as a new design tool for heat exchanger fins that could be additively manufactured. This study goes beyond gradient-based (parametric) topology optimization to fully exploit the freedom in the complexity of the design afforded by AM. In this study, there are no constraints imposed on any of the design parameters beyond the total fin volume. The

[1] Contact author: bkm5207@psu.edu
[2] Now at Naval Air Systems Command
[3] Assistant Professor of Mechanical Engineering.

GA is given the freedom to manipulate the fin dimensions in a way that would maximize the fitness function which is comprised of the total heat rate and pressure drop across the fin.

NOMENCLATURE

A	heat transfer area of offset strip fin surface, m^2
C_p	specific heat, or static pressure coefficient
D_h	hydraulic diameter
dP	pressure drop across fin
F	fitness
f	average Fanning friction factor in the offset strip fin array, $f = \tau_w/(0.5\rho u^2)$
h	height of the offset strip fin channel, or heat transfer coefficient
i	initial population
j	Colburn factor [= $St\ Pr^{2/3}$ or $Nu/(Re\ Pr^{1/3})$]
L_f	length of fin
L_d	length of fluid domain
m	mass flow rate per unit height of fin
N	number of generations
n	population size of one generation
Nu	average overall Nusselt number based on hydraulic diameter
P	static pressure
Pr	Prandtl number
Q	overall heat transfer, $Q = m\ C_p\ (T- T_\infty)$
Re	Reynolds number based on hydraulic diameter
St	Stanton number
s	lateral fin spacing
T	Temperature at the outlet of fluid domain
T_s	wall temperature
T_∞	Temperature at the inlet of the fluid domain
t	fin thickness
u	mass averaged velocity at the outlet of fluid domain
u_∞	velocity at the inlet of fluid domain
Y	width of fluid domain
y	distance along the y-axis

Greek Symbols

α	aspect ratio s/h
γ	ratio t/s
δ	ratio t/L_f

Abbreviations

AM	additive manufacturing
CFD	computational fluid dynamic
GA	genetic algorithms
IMM	initial maximum mutation
IMinM	initial minimum mutation
OSF	offset strip fin
PFHE	plate-fin heat exchanger
TO	topology optimization

2. REVIEW OF RELEVANT LITERATURE

2.1 Offset Strip Fins

Offset strip fins (OSF) are widely used for plate-fin heat exchangers (PFHE). They are especially popular in aerospace applications due to their compactness. A typical OSF has a rectangular cross section cut into small strips of length L_f along the streamwise direction and displaced by about half of the fin pitch in the transverse direction. Fig 1 adapted from [3] shows the construction of a typical OSF. The offset setup leads to periodic interruption of flow which leads to creation of fresh boundary layers and consequent heat transfer improvement. However, interruption of flow also leads to greater pressure drop, manifested by a higher value of effective friction factor. OSFs have been studied by numerous researches over the years [4–8] , however, Kays and London [9] and London and Shah [10] are widely considered the pioneers of OSF research. They established a test program in 1947 at Stanford University for the purpose of developing compact heat exchangers. Their results are found here [9–12]. Manglik and Bergles [3] experimentally investigated the effects of fin geometries as non-dimensional forms on heat transfer and pressure drop. They analyzed 18 different OSF and developed a single continuous expression covering the laminar, transitional, and turbulent flow regimes for both Colburn j-factor (heat transfer) and Fanning friction f-factor (pressure drop).

2.2 Topology Optimization and AM

Since it was first introduced in 1988 by Bendsøe and Kikuchi [13], TO has been extended to many other applications. Its application in the area of structural design has well matured with many literature publications in the last few decades [14–18]. Generally, there are about five different approaches of TO: density, level set, phase field, topological derivative, and evolutionary approaches. The latter is the focus of this study. However, most studies focused on the design of thermo-fluid equipment have used gradient based approaches (the first four). Tsuzuki et al. [19] used CFD to reduce the pressure drop in a zigzag printed circuit heat exchanger by parametrically changing the flow channel configuration to a sine curve. They found that the new configuration reduced the pressure drop to one-fifth that of the zigzag model. Haertel et al. [20] applied density-based topology optimization to design the air-side surface of dry cooled power plant condensers. Their results demonstrate the usefulness of topology optimization to take advantage of the design freedom offered by AM. Dede et al. [21] used gradient-based topology optimization to produce an optimized heat sink for confined jet impingement air cooling and used AM to manufacture it. The experimental results indicate that the optimized AM heat sink design has a higher coefficient of performance (COP) relative to the benchmark plate and pin-fin heat sink. Similar to [21], Saviers et al. [22] successfully used gradient-based methods to generate a non-obvious organic heat exchanger design and built it using AM to demonstrate the manufacturability of organic designs produced by TO. Numerical and experimental results showed that the topology optimized design had 2x less pressure

drop and 2x more heat transfer than the baseline design. Zhao et al. [23] presented a simplified model based on Darcy flow to optimize cooling channels to reduce the intense computational power needed by a full turbulence model in a TO approach.

Gradient based TO methods used for the design of heat exchangers and other complex thermo-fluids equipment are generally based on parametric definition of small to moderate number of constraints, so that the change of the objective function with a change in the design parameter (gradient) can be simply evaluated and the optimization can be fast. However, they can become "trapped" in local minima in the optimization space. Evolutionary methods, such as genetic algorithms are not required to have parametric constraints unless desired by the design problem. All solutions in a population are searched simultaneously, which greatly decreases the probability that the algorithm is trapped in a local optimal solution [24]. They can have a broader search space but can take more resources to evaluate candidate designs.

2.3 Genetic Algorithm

A genetic algorithm uses the concept of natural evolution which removes poor performing designs from the population and allows strong performing designs to stay and create offspring. GAs are classified into two types: single-objective and multi-objective GAs. The single-objective GA aims at maximizing or minimizing a single-objective function created by combining multiple performance variables by optimizing one or more of these variables. Multi-objective GA aims at finding many non-dominated solutions, also called Pareto-Optimal solutions, whose performances spread over the objective function domain. Du et al. [25] used this concept combined with orthogonal design to investigate the characteristics of heat transfer and pressure drop for a PFHE.

There are three typical operators that are used to create new generations in a GA: crossover, mutation and elitism. The crossover operator combines couples of parents to produce offspring. The mutation operator randomly modifies the characteristic of the offspring produced by crossover, to ensure genetic diversity. Elites are the highest performing individuals that will be directly carried over to the next generation. They are used to eliminate regression in performance from one generation to the next. This study employs another operator that is used during the selection process to determine the reproduction pool. This operator is given the term cutoff which is defined as the limit for worse performing individuals that will still get to reproduce.

The use of GA based TO in the design of thermo-fluid devices has not been very well explored, primarily because the coupling between fluid flow and heat transfer is complex and often the resulting geometry is complex and difficult to manufacture. However, the advent of AM and improvement in computational power has allowed for further exploration and development of GA based TO tools. Gosselin et al. [26] reviewed genetic algorithms in the field of heat transfer and concluded that they are becoming increasingly common for optimization problems. Lohn et al. [27] showed that genetic algorithms can be used in conjunction with simulations to create better geometries than traditionally created by a person. Fabbri et al. [28] used 2D CFD in conjunction with a GA to optimize corrugated channels for heat transfer. Dokken and Fronk [29] explored the possibility of combining micro genetic algorithm and CFD to produce optimized liquid cooled heat sinks. A micro-genetic algorithm generally has a population size of about 10 or less and applies the same principles of standard GA, except it does not use a mutation operator. The optimization objective was to minimize the entropy generation which is based on pressure drop and overall thermal resistance. They found that the new model has about 26.4% and 21.7% lower entropy generation rates for the symmetric and non-symmetric power maps, respectively compared to a baseline straight finned cold plate.

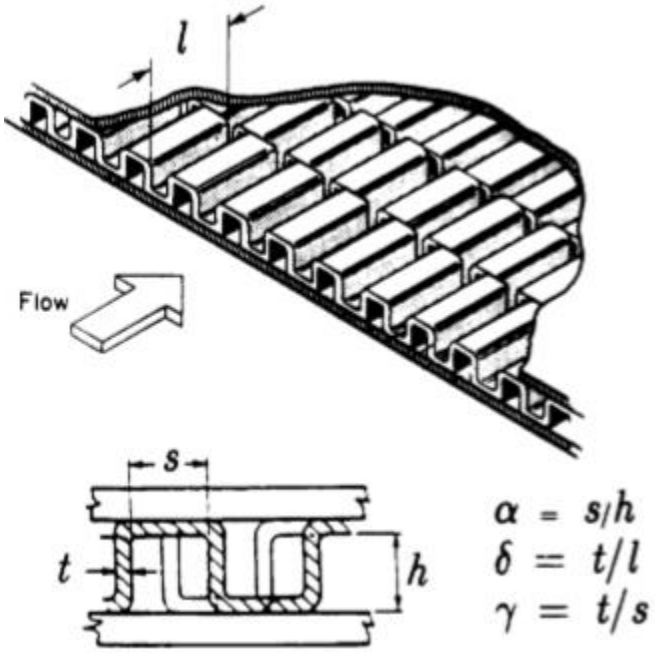

Fig. 1: Description of a typical offset strip fin. Figure adopted from [3].

3. MODELING AND OPIMIZATION METHODOLOGY

The test case chosen here is a 2D model of a single row of an OSF heat exchanger. This is obviously a simple configuration and unrealistic for full heat exchanger applications, but enabled testing of the approach with minimal computational resources.

To allow for a significant parameter space, a rectangular shaped baseline fin geometry was created using voxel representation, where a voxel in the design space is denoted as solid or fluid and can be switched from one to the other by the optimization software. To generate optimal designs, an initial population is generated by mutating the baseline fin a random number of times between the Initial Minimum Mutation (IMinM) and Initial Maximum Mutation (IMM). The population members are then each evaluated in a 2D CFD simulation in OpenFOAM to calculate the performance of each design, as determined by pressure drop and heat transfer. The genetic

algorithm is applied to select best designs, merge them (reproduction), and apply random mutations to generate a new generation. The new generation is re-evaluated in CFD for performance, and the process is repeated for a sufficient number of generations to achieve optimal performance. The process is executed in a Python code with embedded functions that communicate with the CFD evaluation software. The following sections provide details on the GA operations and CFD evaluation.

3.1 Description of Computational Model

The meshed baseline geometry along with the fluid domain are shown in *Fig. 2* below. The size and shape of the fluid domain remains the same for each fin while the fin dimensions will change. The fluid domain is chosen to be 10mm by 3mm with the fin located at its center. Each fin is simulated using a 100x100 rectangular grid mesh. This is shown in Fig. *3* along with boundary conditions. The cyclic boundary shown allows the simulation to act as an infinitely wide array of single fins. The flow is not cyclic in the streamwise direction for this study. Therefore, the fin bank being simulated only has one fin in the streamwise direction. This was done to minimize computation time. Each fin is assumed to be infinitely conductive with a constant surface temperature of 450K. The incoming fluid is at a uniform temperature of 300K and inlet velocity of 3 m/s. The simulations were done using the open source software OpenFOAM. OpenFOAM always operates in a 3-dimensional (3D) Cartesian coordinate system and all geometries are generated in 3D. An empty boundary condition on boundaries normal to the (3rd) dimension is specified in order to solve in 2D. The fluid solver is buoyantBoussinesqSimpleFoam, which is an incompressible, steady-state solver for laminar and turbulent heat transfer problems. A laminar model is used with a Gauss linear gradient scheme for pressure and Bounded Gauss Upwind divergence scheme for all field variables. The Semi-implicit Method for Pressure-linked Equations (SIMPLE) algorithms have been employed to solve for velocity and pressure equations. A Preconditioned (bi-) Conjugate Gradient (PCG) solver with Diagonal incomplete-Cholesky (DIC) preconditioner is used to solve pressure while a Stabilized Preconditioned (bi-) Conjugate Gradient (PBiCGStab) solver with Diagonal incomplete-LU (DILU) preconditioner is used to solve for rest of field variables. The solution converges after 10000 iterations with all the residuals falling under a tolerance value of 10^{-6}.

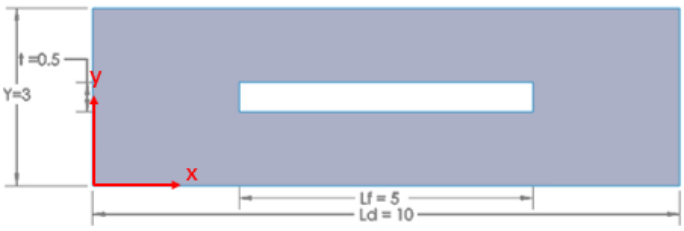

Fig. 2: Dimensions of the baseline geometry and fluid domain.

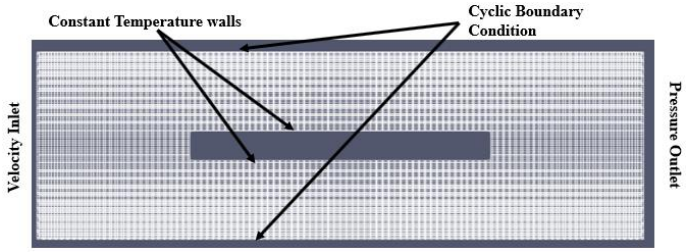

Fig. 3: The meshed baseline fin and fluid domain with the boundary conditions.

3.2 CFD Validation

OpenFOAM was chosen to perform the optimization because of an easy linkage with the GA code through the Python programming language. This allowed for the automation of the entire process and seamless transmission of the new design geometries. Since there are no published results known to the authors that provide heat transfer and pressure drop for a single row OSF, the baseline geometry (shown in *Fig. 2*) was simulated in ANSYS Fluent and the results were used as a benchmark to check the validity of the results obtained by OpenFOAM. This also enabled a determination of the minimum mesh size in OpenFOAM required to properly capture gradients; OpenFOAM did not employ prism layers on the fin surface because of the uniform size voxel approach.

Three mesh sizes were considered in Fluent: 17000, 30000, and 50000 cells. It was found that the solution was independent of the mesh size at all levels, thus a mesh size of 17000 cells was deemed sufficient to act as a benchmark.

The non-dimensional u-velocity and non-dimensional temperature at the outlet of the fluid domain, the overall pressure coefficient, and the overall heat transfer rate from Fluent have been compared to three equivalent mesh sizes from OpenFOAM. *Fig. 4* to *Fig. 8* show these results. It was determined that OpenFOAM grid size of 10000 cells was sufficient to match Fluent and produce grid-independent results for the baseline.

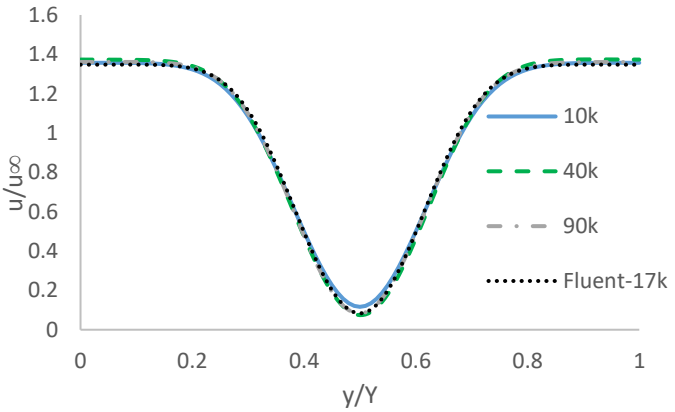

Fig. 4: Non-dimensional u-velocity at the outlet of the fluid domain for three OpenFOAM grids (10k to 90k) and a Fluent grid of 17k.

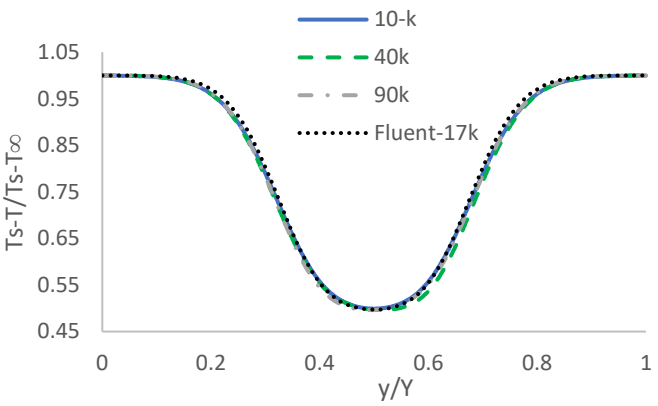

Fig. 5: Non-dimensional temperature at the outlet of the fluid domain for three OpenFOAM grids (10k to 90k) and a Fluent grid of 17k.

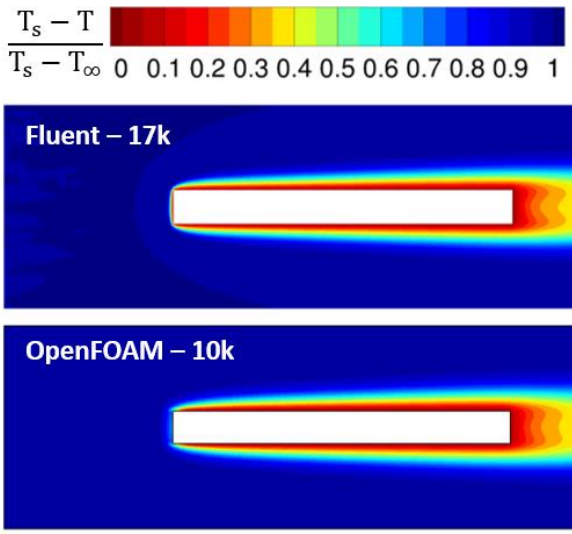

Fig. 6: Non-dimensional temperature contours. Top: Fluent 17k mesh. Bottom: OpenFOAM 10k mesh.

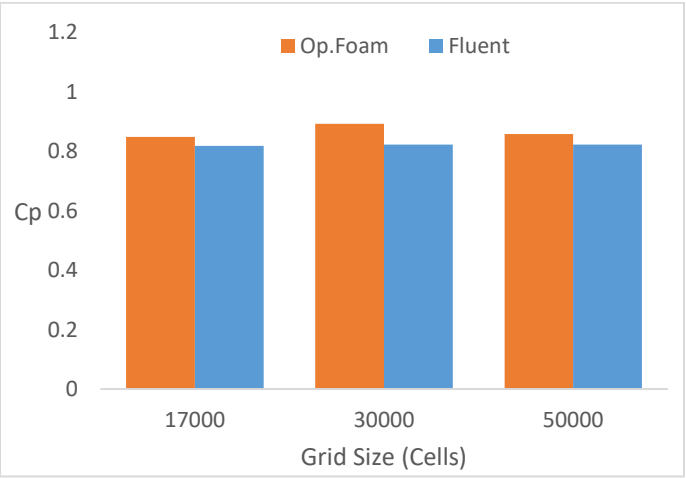

Fig. 7: Static pressure coefficient for three different Fluent and OpenFOAM grids.

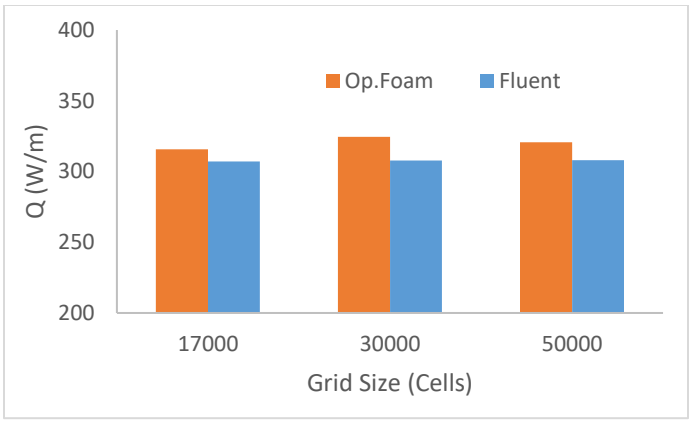

Fig. 8: Total heat transfer per unit fin height for the baseline fin calculated at three different Fluent and OpenFOAM grids.

3.3 Description of GA Procedure

The GA starts with creating the initial generation which has a total of 95 members. The rest of the standard GA parameters that were chosen for this study are listed in *Table 1* below. Each member is generated by mutating the baseline geometry a random number of times between 50 (IMinM) and 2500 (IMM). The domain is divided into a 50x50 grid of voxels. A mutation is defined as randomly changing one voxel that bounds the fin, either by removing or adding it. Only border voxels are subject to mutations. For a voxel to be added it must be a fluid voxel that is adjacent to a solid voxel of the fin. For a voxel to be subtracted it must be a solid voxel that is immediately adjacent to a fluid voxel. When a mutation is invoked it first randomly determines whether the mutation will be an addition or subtraction. After this is determined a voxel is randomly picked. If the chosen voxel fulfills the criterion for either an addition or subtraction the mutation is finished. If not, a new voxel will be chosen and checked until this criterion is fulfilled. There is a condition in the algorithm that prevents voids and ensure that the geometry is a continuous solid.

The performance of each member of the initial population is evaluated in a separate CFD simulation in OpenFOAM. Since the individual evaluations are uncoupled, they are run in parallel. The metrics of interest are the total heat transfer and pressure drop for the fin, where an ideal fin would have infinite heat transfer and zero pressure drop. The overall heat transfer is calculated from the mass flow rate and the change in mass averaged temperature from inlet to exit. Pressure drop is determined using OpenFOAM's pressureDifferencePatch which calculates the difference in average pressures from inlet to outlet. The presence of two objectives would normally require multi-objective optimization, but in this study a composite fitness function is optimized. The definition of fitness (F) below allows for simpler single objective optimization. Note that F is not unitless here.

$$F = \frac{Q}{dP^{1/3}} \frac{[W/m]}{[Pa]} \quad (1)$$

After simulations are successfully completed (as determined by meeting convergence criteria in conservation equation residuals), the designs are ranked by fitness. Then a number of these designs, termed “elites”, will be advanced directly to be part of the next generation. A “cutoff" specifies the number of designs that will get to reproduce, and any designs below the cutoff will be eliminated from the reproduction pool. *Fig*. 9 shows the initial generation produced using the standard parameters. The number on the top left indicates the fitness and the number on top right represents the design number which is used to track the generation the design is emerged from.

The second step is to generate the second generation. The number of members that need to be created for the second generation is equal to the total population (95) minus the number of elites. There are three different mechanisms to achieve this. The first is to randomly select a member of the post-selection population and mutate it up to 150 times, in the same manner as described for the initial design generation. There is a one in three chance that a smoothing algorithm will also be applied in this mechanism. The second mechanism takes two parents and does a voxel by voxel comparison. The resultant geometry only has voxels that both parents have in common. A random number of mutations up to 50 is then applied to the resultant geometry. *Fig. 10* shows the second reproduction mechanism. The final mechanism is similar to the second one except it uses any voxel that is contained by either parent to create the child geometry.

The GA will start over again by evaluating the new population in CFD followed by the selection process and reproduction/mutation. This process is repeated for 60 generations, which was determined by the asymptotic behavior of the performance and the need to limit the GA from running indefinitely. *Fig. 11* below describes the step of the GA approach used here.

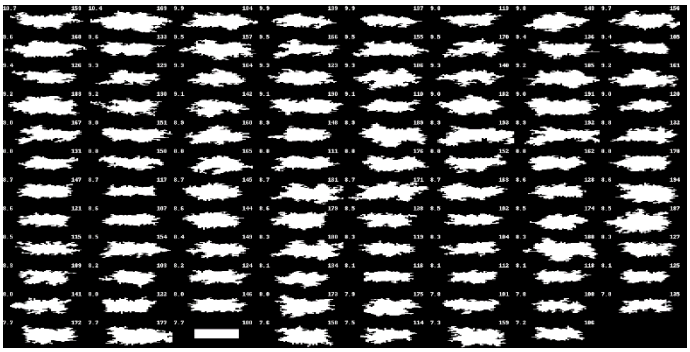

Fig. 9: Variation of the initial population produced by the standard GA parameters.

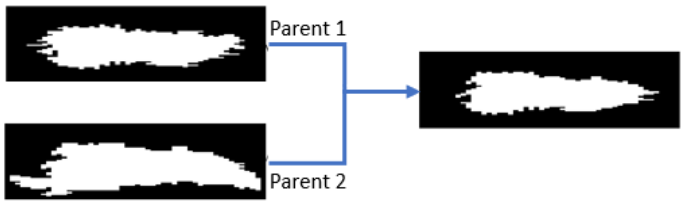

Fig. 10: The second GA reproduction mechanism, where only the “genes” (solid voxels) of both parents are kept in the child.

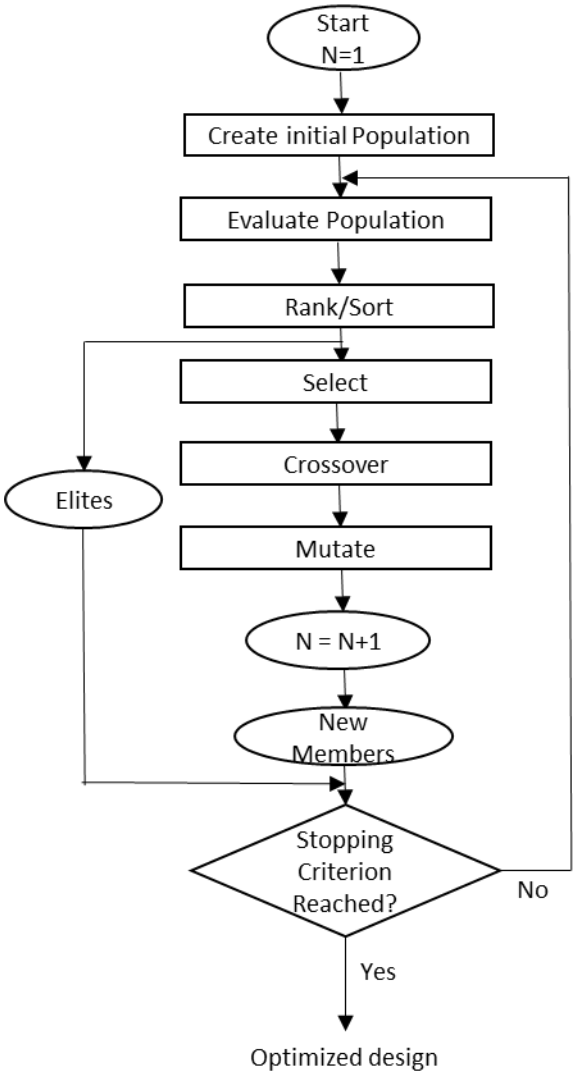

Fig. 11: Description of genetic algorithm approach used here.

Table 1: Standard GA Parameters

n	Elites	Cutoff	IMM/IMinM
95	15	25	2500/50

4. RESULTS AND DISCUSSION

The GA was initially run for nominal conditions of Re = 900 and the standard parameters in Table 1 above, for 60 total generations. *Fig. 12* illustrates how the algorithm converges to a best design at about this number of generations. The graph depicts the best performance, average performance, and each individual performance result as a function of generation number. As the generations progress, asymptotic behavior of the best and the average fitness value can be observed. After 60 generations, the GA produced a geometry that performed over 60% better than the baseline rectangular fin from which the algorithm started. The baseline geometry and the new optimized fin are shown in *Fig. 13* below. The optimized fin shows an interesting type of sinusoidal shape. This shape has been

observed for the standard GA parameters as well as the different variations of parameters as explained in the next section. The extension of the nose and tail is also interesting. It appears as though the extensions increase surface area with very little pressure loss penalty. At generation 60 this geometry had taken over the entire population. This geometry may also possibly be easier to manufacture due to the uniform, thicker edges.

Fig. 14 is a Pareto chart for the nominal GA result, with pressure drop on the horizontal axis and heat transfer on the vertical axis. The various designs are colored by generation number, starting with dark colors and progressing to lighter colors toward generation number 60. The resultant population shows a clear tradeoff between pressure drop and heat transfer. The best designs all lie on the upper leftmost front of this grouping. Even though there was a single objective function, the algorithm clearly produces a range of optimal designs that would achieve high overall performance.

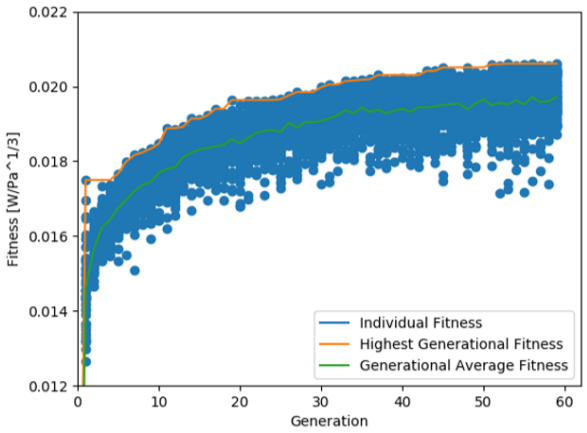

Fig. 12: The individual, average, and max fitness of each generation.

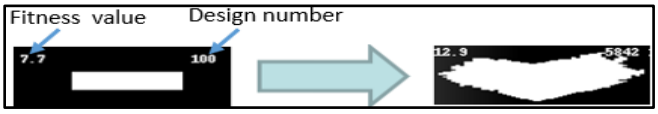

Fig. 13: The baseline fin (left) and the new optimized fin.

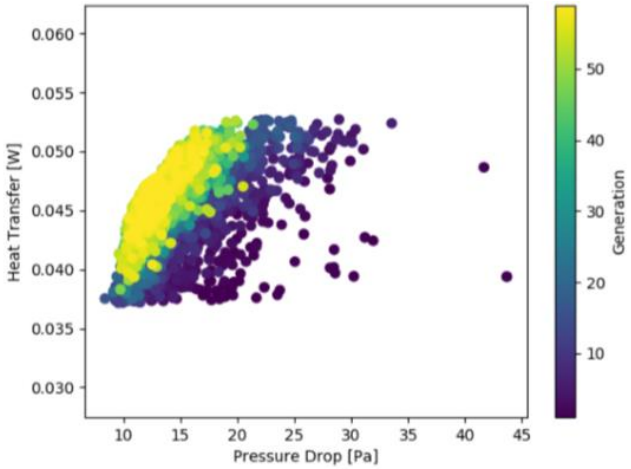

Fig. 14: The Pareto front of optimal pressure drop or heat transfer that develops from the GA with increasing number of generations.

4.1 GA Sensitivity to Change in Parameters

It is important to understand the effect of changing the various GA parameters on the speed of convergence and most importantly the shape of the optimized fin. Thus, each one of the four important GA parameters in *Table 1* have been varied one at a time while the other parameters were kept constant and the results are discussed below.

Effect of Initial Mutation Rate

Initial maximum mutation (IMM) and initial minimum mutation (IMinM) have a great effect on the speed of the GA code. This parameter is related only to the mechanism by which the production of initial generation designs happens- The baseline fin is randomly mutated by a number greater than IMinM at minimum and up to a number equal to IMM. The process is repeated until all the 95 members of the initial generation are generated.

Low mutation rates mean the GA will spend less time creating the initial generation, but this will require a higher number of generations (the stopping criterion) for the GA to converge (because the initial generation is not very diverse).

A very high IMM/IMinM is also not good because it results in longer time to create the initial generation with little gain to the convergence process. This is because there is a certain limit of diversity for every member of the initial generation beyond which more mutation will not necessarily result in higher performance. A range of IMM/IMinM has been tested and based on observations it was concluded that IMM/IMinM of 2500/50 is appropriate.

Effect of Population Size

A range of population size between 20 and 180 has been tested. A population size of 50 gives a geometry (and maximum fitness) that is trending towards the geometry obtained with population size of 95 as seen in *Fig. 15* which represents the variation of the maximum fitness with the change in population size. The same trending behavior has been observed for population size of 20 but to a lesser degree when compared to population size of 50. These results are in line with the assumption that large population size results in better performing children, due to increased genetic diversity. Based on this result, population sizes of 120, 150, and 180 were also tested. The results from these higher population sizes showed little improvement over the standard population size of 95, with the fitness values from the optimal design fluctuating around a nominal level of 13.1. This suggests that increasing the population size beyond this value will not result in significant improvement in fitness and will only increase processing time.

Effect of Cutoff

Minimizing the cutoff, which is the number of members that stay for the next generation to be part of the reproduction pool, gave the most interesting results. When this number is set to 12, it resulted in a sinusoidal geometry with uniform thickness. The nose and tail pattern have been replaced by a very uniform vertical edge. However, repeatability of this geometry was

inconsistent. A cutoff value of 50 also gave sinusoidal shape but with no improvement in performance relative to the nominal value. *Fig. 16* shows the effect of varying cutoff on the fitness value along with the resulting geometries.

Effect of Elites

When the number of elites is reduced to 5, the resulting geometry is similar to that for 15 elites, but without the long nose and a slightly lower fitness value. Elites 5 and 50 gave no improvement from the nominal elites = 15, however, elites = 30 gave the most interesting results, similar to the sinusoidal shape observed from varying cutoff. Running the GA with elites = 30 and without changing the cutoff (kept at 25) has the same effect of lowering cutoff to 12, but with the advantage of reducing the simulation time by up to 2 hours since the GA will have to generate less members. The effect of varying the elites along with the resulting geometries is presented in *Fig. 17*.

Figures 14 through 16 show that the change in the population size seems to be very important for the convergence of the GA since the variation in the fitness value is the greatest (between 11.7 and 13.4 as the population size increases). Change in the number of elites was not critical as evident by the limited change in the optimal fitness values. The GA is also not very sensitive to the cutoff. However, the concept of cutoff is very important to the GA in the sense that it needs a way to filter out bad performing members and prevent them from reproducing.

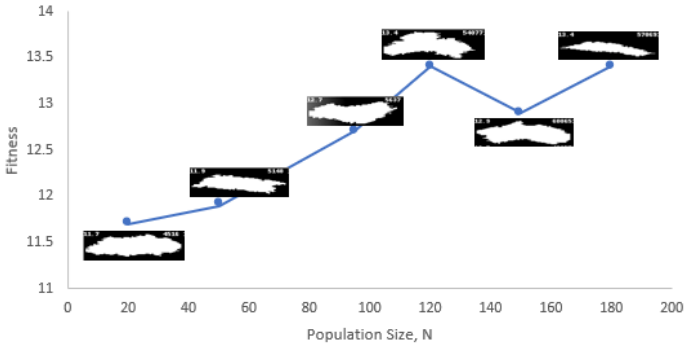

Fig. 15: Variation in the optimal fitness value resulting from varying population size.

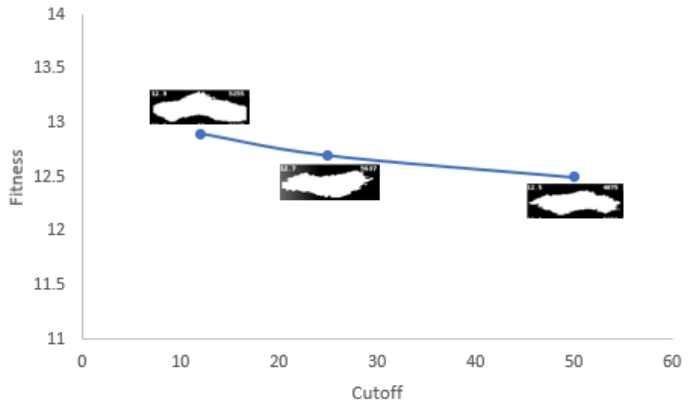

Fig. 16: Variation in the optimal fitness value resulting from varying the cutoff.

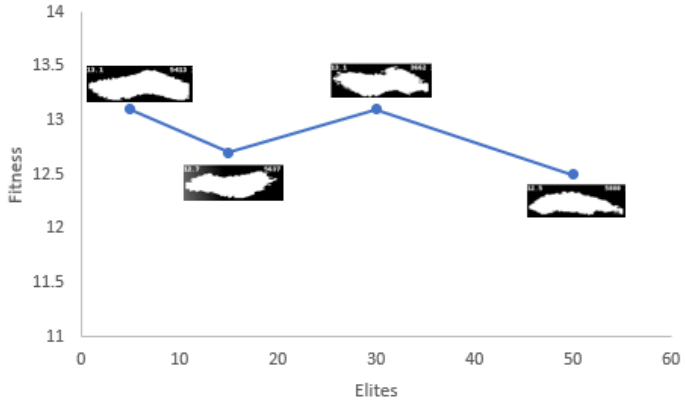

Fig. 17: Variation in the optimal fitness value resulting from varying the number of elites.

4.2 Effect of Reynolds Number

This study tested multiple inlet velocities in the range of $0.835 \text{ m/s} \leq u_\infty \leq 33.33 \text{ m/s}$ ($93 \leq Re \leq 3712$) and compared the numerical results of the optimized fins to the numerical results of the baseline fin and the j and f factor correlations for OSF developed by Manglik and Bergles [3]. The results are plotted in a logarithmic scale in terms of the corresponding Re numbers based on the hydraulic diameter to make it consistent with [3]. Note that the Manglik and Bergles correlations used here are continuous expressions covering the laminar, transitional, and turbulent flow regimes. Since the flow regime in this study is laminar, only the relevant Re range has been plotted.

The j and f factors from the CFD have been calculated using the formulas provided in the nomenclature section. Recall that the simulations in this study were only in 2D.

The slope of the j-factor of the baseline fin in *Fig. 18* is similar to the correlation of Manglik Bergles but has a lower value. This might be because only one row has been simulated in the case of the baseline fin as opposed to multiple rows in the correlation case which enhances the heat transfer. At lower Re numbers, the baseline f-factor in *Fig. 19* is also lower than the OSF correlation but it increases with the increase of Re number and exceeds the OSF correlation at maximum Re. This behavior can be explained by the morphological difference between the solid fins simulated in this study and the OSF shown in *Fig. 1*. Note also that Manglik and Bergles reported that there is greater scatter in f data compared to j data due to manufacturing variations which implies that the accuracy of the f-factor correlation is limited [3].

Aligned with the expectations from the earlier discussion, *Fig. 18* shows that the new optimized fins' heat transfer performance is superior to the baseline and slightly lower than the correlation of Manglik and Bergles. The average improvement in the j-factor of the optimized fins is about 0.75 times the baseline j-factor. Likewise, the pressure drop in the optimized fins is very high as evident by the f-factor presented in *Fig. 19*. The ratio of the optimized fin j-factor relative to the baseline fin j-factor has been plotted against the ratio of the optimized fin f-factor to the f-factor of the baseline fin at various Re numbers as presented in *Fig. 20*. It appears that the

performance of the optimized fin improves with the increase in Re Number.

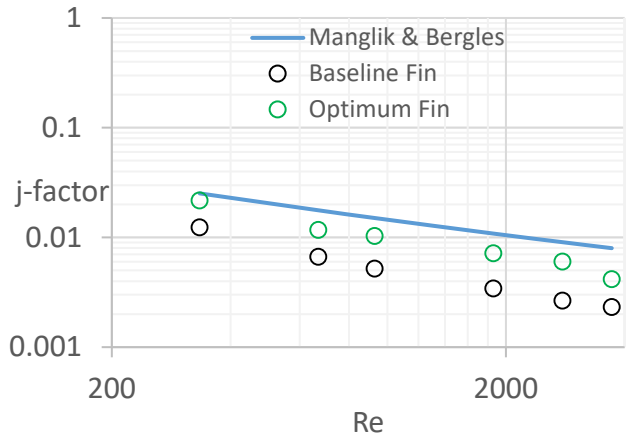

Fig. 18: j-factor of the optimized fin compared to the baseline fin and the empirical formula provided by Manglik & Bergles.

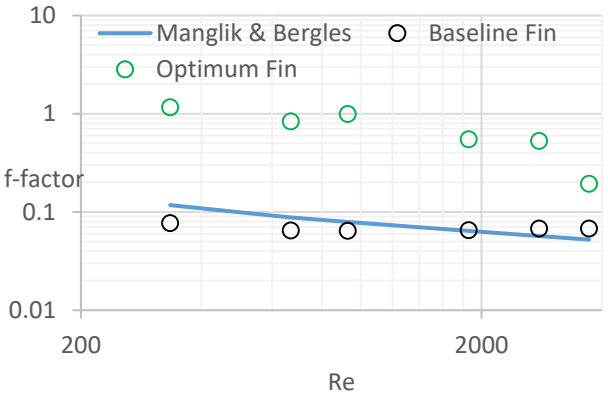

Fig. 19: f-factor of the optimized fin compared to the baseline fin and the empirical formula provided by Manglik & Bergles

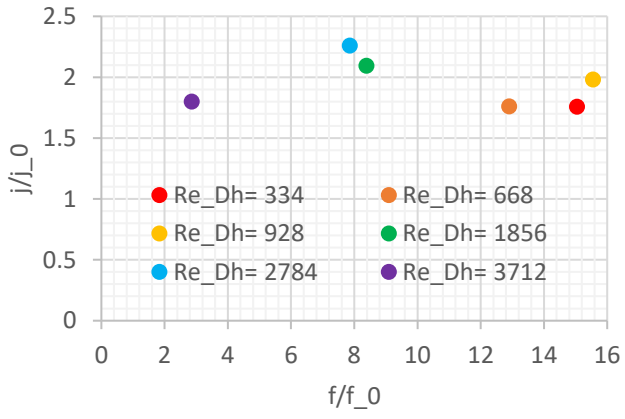

Fig. 20: j-factor ratio vs f-factor ratio

5. CONCLUSION

This study demonstrated the ability to combine GA based TO and CFD to generate organic heat exchanger fin designs. The new optimized fin has 60% performance improvement over the rectangular baseline geometry. The study also investigated the effect of varying the GA parameters. It was found that varying population size has the greatest effect on the performance of the GA, and a minimum size is required to achieve high fitness. It was also found that population size of 95, number of elites equal to 30, and a cutoff of 25 give the best results in terms of minimal processing time but high optimized fin performance.

The effect of varying flow Reynolds number has also been tested and the j- and f-factor of the optimized fins have been evaluated and compared to those from the baseline and OSF correlations. The j-factor results show that the optimized fins outperformed the baseline, however, this comes with the cost of high pressure drop. The ratio of j-factor enhancement to f-factor penalty seems to decrease with increasing Reynolds number, suggesting that the design approach here may be more effective for high Reynolds number operation.

The intent of the voxel-based design process demonstrated here is to align with the digital representation of geometry in a powder bed fusion AM process. It should be noted that no manufacturing constraints have been considered yet, and so the optimal geometries may have features that would be too thin to fabricate reliably. However, manufacturing constraints can easily be incorporated in the GA process.

Because of the large number of computations currently required (95 CFD simulations per generation for up to 60 generations), this study was initially limited to 2D and a single row of fins. The computing power required will increase by orders of magnitude if 3D fins and multiple rows of fins are considered. While this is not impossible to achieve, it does suggest that some simplifications to the GA approach (perhaps surrogate design surfaces, or B-spline definition of the fin perimeter) might be warranted. Overall, the approach presented here is unique in its ability to generate freeform designs that may be achievable with AM.

ACKNOWLEDGEMENTS

The authors would like to acknowledge the use of the Pennsylvania State University's Institute for CyberScience Advanced CyberInfrastructure (ICS-ACI) for the high-performance computing presented here.

REFERENCES

[1] Shah, R. K., and Webb, R. L., 1983, "Compact and Enhanced Heat Exchangers," Heat Exch. Theory Pract. J. Taborek, pp. 425–468.

[2] Dbouk, T., 2017, "A Review about the Engineering Design of Optimal Heat Transfer Systems Using Topology Optimization," Appl. Therm. Eng., **112**, pp. 841–854.

[3] Manglik, R. M., and Bergles, A. E., 1995, "Heat Transfer and Pressure Drop Correlations for the Rectangular Offset Strip Fin Compact Heat Exchanger," Exp. Therm. Fluid Sci., **10**(2), pp. 171–180.

[4] Wieting, A. R., 1975, "Empirical Correlations for Heat Transfer and Flow Friction Characteristics of Rectangular Offset-Fin Plate-Fin Heat Exchangers," J. Heat Transfer, **97**(3), p. 488.

[5] Joshi, H. M., and Webb, R. L., 1987, "Heat Transfer and Friction in the Offset Stripfin Heat Exchanger," Int. J. Heat Mass Transf., **30**(1), pp. 69–84.

[6] Mochizuki, S., Yagi, Y., and Yang, W. J., 1988, "Flow Pattern and Turbulence Intensity in Stacks of Interrupted Parallel-Plate Surfaces," Exp. Therm. Fluid Sci., **1**(1), pp. 51–57.

[7] Dubrovsky, E. V., and Vasiliev, V. Y., 1988, "Enhancement of Convective Heat Transfer in Rectangular Ducts of Interrupted Surfaces," Int. J. Heat Mass Transf., **31**(4), pp. 807–818.

[8] Guo, J., Xu, M., and Cheng, L., 2009, "The Application of Field Synergy Number in Shell-and-Tube Heat Exchanger Optimization Design," Appl. Energy, **86**(10), pp. 2079–2087.

[9] Kays, W. ., and London, A. L., 1984, *Compact Heat Exchanger*, McGraw-Hill, Inc., New York.

[10] London, A. L., and Shah, R. K., 1968, "Offset Rectangular Plate-Fin Surfaces—Heat Transfer and Flow Friction Characteristics," J. Eng. Gas Turbines Power, **90**(3), p. 218.

[11] Kays, W. M., 1960, "The Basic Heat Transfer and Flow Friction Characteristics of Six Compact High-Performance Heat Transfer Surfaces," J. Eng. Power, **82**(1), p. 27.

[12] Briggs, D. C., and London, A. L., 1961, "The Heat Transfer and Flow Friction Characteristics of Five Offset Rectangular and Six Plain Triangular Plate-Fin Heat Transfer Surface," *International Development in Heat Transfer, ASME*, pp. 122–134.

[13] Bendsoe, M. P., and Kikuchi, N., 1988, "Generating Optimal Topologies in Structural Desing Using A Homogenization Method," Comput. Methods Appl. Mech. Eng., **71**, pp. 197–224.

[14] Hassani, B., and Hinton, E., 1998, "A Review of Homogenization and Topology Optimization I - Homogenization Theory for Media with Periodic Structure," Comput. Struct., **69**(6), pp. 707–717.

[15] Hassani, B., and Hinton, E., 1998, "A Review of Homogenization and Topology Opimization II - Analytical and Numerical Solution of Homogenization Equations," Comput. Struct., **69**(6), pp. 719–738.

[16] Eschenauer, H. A., and Olhoff, N., 2003, "Topology Optimization of Continuum Structures: A Review," Appl. Mech. Rev., **54**(4), p. 331.

[17] Liang, Q. Q., 2007, "Performance-Based Optimization : A Review," **10**(6), pp. 739–753.

[18] Sigmund, O., and Maute, K., 2013, "Topology Optimization Approaches," Struct. Multidiscip. Optim., **48**(6), pp. 1031–1055.

[19] Tsuzuki, N., Kato, Y., and Ishiduka, T., 2007, "High Performance Printed Circuit Heat Exchanger," Appl. Therm. Eng., **27**(10), pp. 1702–1707.

[20] Haertel, J. H. K., and Nellis, G. F., 2017, "A Fully Developed Flow Thermofluid Model for Topology Optimization of 3D-Printed Air-Cooled Heat Exchangers," Appl. Therm. Eng., **119**.

[21] Dede, E. M., Joshi, S. N., and Zhou, F., 2015, "Topology Optimization, Additive Layer Manufacturing, and Experimental Testing of an Air-Cooled Heat Sink," J. Mech. Des., **137**(11), p. 111403.

[22] Saviers, K. R., Ranjan, R., and Mahmoudi, R., 2019, "Design and Validation of Topology Optimized Heat Exchangers," *AIAA Sci-Tech Forum*, pp. 1–7.

[23] Zhao, X., Zhou, M., Sigmund, O., and Andreasen, C. S., 2018, "A 'Poor Man's Approach' to Topology Optimization of Cooling Channels Based on a Darcy Flow Model," Int. J. Heat Mass Transf., **116**, pp. 1108–1123.

[24] Wei, G., 2003, "An Improved Fast-Convergent Genetic Algorithm," *Proceedings of the 2003 IEEE. Intemational Conference on Robotics,Intelligent Systems and Signal Processing*, pp. 1197–1202.

[25] Du, J., Yang, M. N., and Yang, S. F., 2016, "Correlations and Optimization of a Heat Exchanger with Offset Fins by Genetic Algorithm Combining Orthogonal Design," Appl. Therm. Eng., **107**, pp. 1091–1103.

[26] Gosselin, L., Tye-Gingras, M., and Mathieu-Potvin, F., 2009, "Review of Utilization of Genetic Algorithms in Heat Transfer Problems," Int. J. Heat Mass Transf., **52**(9–10), pp. 2169–2188.

[27] Lohn, J. D., Linden, D. S., Hornby, G. S., Kraus, W. F., and Seufert, S. E., 2004, "Evolutionary Design of an X-Band Antenna for NASA's Space Technology 5 Missio," *IEEE Antennas and Propagation Society Symposium*, IEEE, pp. 2313–2316.

[28] Fabbri, G., 1997, "A Genetic Algorithm for Fin Profile Optimization," Int. J. Heat Mass Transf., **40**(9), pp. 2165–2172.

[29] Dokken, C. B., and Fronk, B. M., 2018, "Optimization of 3D Printed Liquid Cooled Heat Sink Designs Using a Micro-Genetic Algorithm with Bit Array Representation," Appl. Therm. Eng., **143**(July), pp. 316–325.